Available online at www.sciencedirect.com

ScienceDirect

Geochimica et Cosmochimica Acta 223 (2018) 364–376

Geochimica et Cosmochimica Acta

www.elsevier.com/locate/gca

Diffusion coefficients of Mg isotopes in $MgSiO_3$ and Mg_2SiO_4 melts calculated by first-principles molecular dynamics simulations

Xiaohui Liu [a,b], Yuhan Qi [c], Daye Zheng [a,b], Chen Zhou [c], Lixin He [a,b,*], Fang Huang [c,*]

[a] Key Laboratory of Quantum Information, University of Science and Technology of China, Hefei, Anhui 230026, China
[b] Synergetic Innovation Center of Quantum Information and Quantum Physics, University of Science and Technology of China, Hefei 230026, China
[c] CAS Key Laboratory of Crust-Mantle Materials and Environments, School of Earth and Space Sciences, University of Science and Technology of China, Hefei, Anhui 230026, China

Received 6 May 2017; accepted in revised form 8 December 2017; Available online 14 December 2017

Abstract

The mass dependence of diffusion coefficient (D) can be described in the form of $\frac{D_i}{D_j} = \left(\frac{m_j}{m_i}\right)^{\beta}$, where m denotes masses of isotope i and j, and β is an empirical parameter as used to quantify the diffusive transport of isotopes. Recent advances in computation techniques allow theoretically calculation of β values. Here, we apply first-principles Born-Oppenheimer molecular dynamics (MD) and pseudo-isotope method (taking $\frac{m_j}{m_i} = \frac{1}{24}, \frac{6}{24}, \frac{48}{24}, \frac{120}{24}$) to estimate β for $MgSiO_3$ and Mg_2SiO_4 melts.

Our calculation shows that β values for Mg calculated with ^{24}Mg and different pseudo Mg isotopes are identical, indicating the reliability of the pseudo-isotope method. For $MgSiO_3$ melt, β is 0.272 ± 0.005 at 4000 K and 0 GPa, higher than the value calculated using classical MD simulations (0.135). For Mg_2SiO_4 melt, β is 0.184 ± 0.006 at 2300 K, 0.245 ± 0.007 at 3000 K, and 0.257 ± 0.012 at 4000 K. Notably, β values of $MgSiO_3$ and Mg_2SiO_4 melts are significantly higher than the value in basalt-rhyolite melts determined by chemical diffusion experiments (0.05). Our results suggest that β values are not sensitive to the temperature if it is well above the liquidus, but can be significantly smaller when the temperature is close to the liquidus. The small difference of β between silicate liquids with simple compositions of $MgSiO_3$ and Mg_2SiO_4 suggests that the β value may depend on the chemical composition of the melts. This study shows that first-principles MD provide a promising tool to estimate β of silicate melts.

Keywords: Stable isotopes; Diffusion; Silicate melt; First-principles

1. INTRODUCTION

Stable isotopes provide a fundamental tool which has been extensively used to study geochemical processes. Isotopes can be fractionated by thermodynamic equilibrium exchange reactions between phases with different chemical activities and energy (Urey, 1947). Mass-dependent equilibrium isotope fractionation can dramatically decrease with increasing temperature (Bigeleisen and Mayer, 1947;

* Corresponding authors at: Key Laboratory of Quantum Information, University of Science and Technology of China, Hefei, Anhui 230026, China (L. He) and CAS Key Laboratory of Crust-Mantle Materials and Environments, School of Earth and Space Sciences, University of Science and Technology of China, Hefei, Anhui 230026, China (F. Huang).

E-mail addresses: helx@ustc.edu.cn (L. He), fhuang@ustc.edu.cn (F. Huang).

https://doi.org/10.1016/j.gca.2017.12.007
0016-7037/

Urey, 1947). Stable isotopes can also be fractionated due to kinetic effect, which results from the mass dependence of the molecular velocity during mass transport (e.g. Van Orman and Krawczynski, 2015; Gausonne et al., 2016). Kinetic isotope fractionation can be caused by chemical and thermal diffusion or other physical transport processes such as evaporation and disequilibrium crystallization (e.g. Young et al., 2002; Knight et al., 2009; Richter et al., 2009a; Huang et al., 2009, 2010; Dauphas et al., 2010; Teng et al., 2011). Large isotope fractionations caused by kinetic processes were widely observed in high temperature processes in recent studies on both laboratory experiments and natural rocks (e.g. Richter et al., 2003, 2008; Lundstrom et al., 2005; Beck et al., 2006; Teng et al., 2006; Rudnick and Ionov, 2007; Watkins et al., 2009; Wu et al., 2017).

Because diffusion-driven isotope fractionations vary with time and will eventually approach to thermal dynamic equilibrium, diffusive isotope fractionations recorded in rocks and minerals provide unique temporal constrains on geological processes (e.g. Beck et al., 2006; Dauphas, 2007; Parkinson et al., 2007; Chopra et al., 2012; Oeser et al., 2015; Sio and Dauphas, 2017). In a common case of diffusion process, isotope fractionations reflect the difference of diffusivities of isotopes which are dependent on their atom masses (e.g. Richter et al., 1999, 2003). In the studies of mass dependence of diffusion coefficients (D), D of isotopes of the same element is commonly parameterized as:

$$\frac{D_i}{D_j} = \left(\frac{m_j}{m_i}\right)^{\beta} \quad (1)$$

where m_i and m_j are the masses of two isotopes and β is an empirical scaling exponent which ranges from 0 and 0.5 (e.g. Richter et al., 1999; Watson and Baxter, 2007). Specifically, a β of 0.5 stands for the case of an ideal monatomic gas system.

The kinetic isotope effects caused by diffusion in silicate melts have been addressed in the literature (e.g. Richter et al., 1999, 2003, 2008, 2009b; Watkins et al., 2009, 2011, 2014). Richter et al. (1999) investigated isotope diffusion in silicate melts, and reported $\beta \leq 0.025$ for Ge isotope diffusion in molten GeO_2, and $\beta = 0.05$–0.1 for Ca isotopes diffusion in CaO-Al_2O_3-SiO_2 melts. These experiments showed that stable isotopes could be significantly fractionated in silicate melts at high temperature. Richter et al. (2003, 2008, 2009b) and Watkins et al. (2009) showed that β values for Ca, Mg, and Fe ($\beta \approx 0.05 \pm 0.05$) were smaller than Li ($\beta \approx 0.22$) in natural silicate melts (e.g. basalt-rhyolite and ugandite-rhyolite) by diffusion-couple experiments. Watkins et al. (2011, 2014) studied diffusive Mg and Ca isotope fractionations in silicate melts, showing that β factors can be highly variable in different liquid compositions, and isotopic fractionations by diffusion depend on the direction of diffusion in composition space. These experimental results show that the β correlates with the solvent-normalized diffusivity, and higher β factors tend to occur in silicate melts with higher content of $SiO_2 + Al_2O_3$ (Watkins et al., 2017). Experiment studies provide reliable observations for diffusive isotope fractionation in silicate melts, while theory calculations represent an important complement for understanding the mechanisms controlling kinetic isotope fractionations.

Recent advances in computation technique provide a novel method to theoretically calculate β values. Classical MD with empirical potential has been used to study the isotope effect on diffusion in liquids, such as MgO melts (Tsuchiyama et al., 1994), and liquid water (e.g. Bourg and Sposito, 2007, 2008; Bourg et al., 2010). Only recently, Goel et al. (2012) calculated β values for silicate melt using LAMMPS (Plimpton, 1995) and GROMACS (Hess et al., 2008). They estimated β of 0.135 at 1 atm for Mg isotopes in $MgSiO_3$ melt and β of 0.05 for Si isotopes in SiO_2 and $MgSiO_3$ melt (Goel et al., 2012), suggesting that large diffusive isotope effects persist even at extremely high temperatures. The atomistic simulations based on force fields can be used to study diffusion in melts of large system sizes and in long time scales. However, force fields need empirical inputs that are either from experiments or first-principles calculations, and the prediction power of such force fields needs to be rigorously addressed via systematic tests. Therefore, further theoretical studies are still required to investigate the kinetic isotope fractionation in silicate melts.

Density functional theory (DFT), a first-principles method based on quantum mechanics, has been increasingly used to predict properties of various materials. Generally, ions diffusion in liquid state involves forming and breaking of chemical bonds, which is difficult to be treated at the empirical force field level. In this case, the first-principles MD (FPMD) provides a reliable tool to study kinetic isotope fractionation. Here we use the FPMD method to obtain the mass dependence of self-diffusion coefficients of Mg isotopes in $MgSiO_3$ and Mg_2SiO_4 melts which are important components in igneous systems. Especially, the FPMD method can accurately describe the formation and breakage of the chemical bonds compared to classical MD. Our simulations were performed at above 2300 K and 0 GPa, different with the conditions in the previous experimental studies with lower temperature but higher pressure. The purpose of this study is to provide a theoretical approach to calculate β values of isotopes in melts and give new insight into the temperature and composition effects on Mg isotopes diffusivities in silicate melts.

2. METHODS

The diffusion properties of $MgSiO_3$ and Mg_2SiO_4 are studied via the FPMD based on DFT within local density approximation (LDA). All FPMD simulations in this study were carried out with the ABACUS (Atomic-orbital Based Ab-initio Computation at USTC) package (Li et al., 2016), which was developed to perform large-scale DFT simulations using linear combinations of atomic orbitals (LCAO) method (Chen et al., 2010, 2011). The recently developed systematically improvable optimized numerical atomic orbitals (Chen et al., 2010, 2011) are an excellent approach to describe various materials such as molecules, crystalline solids, surfaces, and defects (Li et al., 2016). We adopt norm-conserving pseudopotentials (Giannozzi et al., 2009) for Mg, Si, and O. The energy cutoff used in simulations

is 80 Ry. The atomic orbitals basis set of Mg includes two *s*, and one polarized *p* orbitals (2*s*1*p*), and the basis sets of Si and O were chosen to be two *s*, two *p*, and one polarized *d* orbitals (2*s*2*p*1*d*). The radii cutoffs of numerical atomic orbitals are 7 bohr for Mg, 6 bohr for both Si and O.

For $MgSiO_3$ liquid, simulations were carried out in an orthogonal cell containing 160 atoms (32 formula units), with periodic boundary conditions in all three dimensions. The volume of the cell was set to 38.9 cm^3/mol – the experimental value for liquid at ambient melting point 1830 K (Lange and Carmichael, 1987). For Mg_2SiO_4 liquid, the orthogonal cell contains 224 atoms (32 formula units), and the reference volume is 52.36 cm^3/mol – an estimated volume (Lange and Carmichael, 1987; Bowen and Andersen, 1914) at the ambient melting temperature of 2163 K. For both $MgSiO_3$ and Mg_2SiO_4 liquids, the canonical ensemble (constant number of particles N, constant volume V, and constant temperature T) was used. The initial liquid configurations were prepared by melting the structures at 6000 K for $MgSiO_3$ and 8000 K for Mg_2SiO_4 for 2 ps, and then equilibrating the systems to lower temperatures. For all FPMD simulations, the time step was set to be 1 fs, and the total simulation ran up to 60 ps.

To determine the diffusive isotope effects with sufficient precision, MD simulations were always carried out at high temperature and with an artificially pseudo-mass contrast between isotopes of the same element (Goel et al., 2012). In this study, we carried out simulations at 2300 K, 3000 K, and 4000 K for Mg_2SiO_4 liquid, and simulations at 4000 K for $MgSiO_3$ liquid. We have used pseudo-masses of Mg isotopes with atomic mass $M^* = 1$, 6, 48, 120 g/mol, i.e., the mass ratios relative to ^{24}Mg range from 1/24 to 120/24. The pseudo-mass method has been used in studying the isotopic mass dependence of diffusion in aqueous solutions via MD simulations, and the results were in good agreement with experimental data (Bourg et al., 2010).

Our FPMD results were fitted to the third-order Birch-Murnaghan isothermal equation of state (EOS) (1947):

$$P(V) = \frac{3K_0}{2}\left[\left(\frac{V_0}{V}\right)^{\frac{7}{3}} - \left(\frac{V_0}{V}\right)^{\frac{5}{3}}\right]\left\{1 + \frac{3}{4}(K_0' - 4)\left[\left(\frac{V_0}{V}\right)^{\frac{2}{3}} - 1\right]\right\} \quad (2)$$

where P and V are the pressure and volume, respectively. V_0, K_0, and K_0' are the equilibrium volume, isothermal bulk modulus, and its first pressure derivative, respectively.

We analyzed the structural and dynamical properties of liquid $MgSiO_3$ and Mg_2SiO_4 systems. The self-diffusion coefficients (D_α) of element α in liquids were calculated from the mean square displacement (MSD) using the Einstein relation (Einstein, 1956):

$$D_\alpha = \lim_{t\to\infty} \frac{\langle|\vec{r}(t+t_0) - \vec{r}(t_0)|^2\rangle_\alpha}{6t} \quad (3)$$

Here $\vec{r}(t)'s$ are the particle trajectories, and $\langle\ldots\rangle_\alpha$ denotes an average of MSD over all atoms of type α and over time with different origins $t_0's$. The radial distribution function g(r) is calculated based on

$$g(r) = \frac{1}{\rho N}\left\langle \sum_{i=1}^{N}\sum_{j=1,j\neq i}^{N} \delta(\vec{r} - \vec{R}_i + \vec{R}_j)\right\rangle \quad (4)$$

where ρ and N are the ionic density and total number of atoms, respectively, and $\vec{R}$ is atomic coordinate. The partial radial distribution function (Marrocchelli et al., 2010) between two species *a* and *b* can be written as:

$$g_{ab}(r) = \frac{N}{\rho N_a N_b}\left\langle \sum_{i=1}^{N_a}\sum_{j=1}^{N_b} \delta(\vec{r} - \vec{R}_i^a + \vec{R}_j^b)\right\rangle \quad (5)$$

We adopted a decay function $H(t)$ to compute the lifetimes of the bonds between different species of atoms in $MgSiO_3$ and Mg_2SiO_4 liquids. The decay function represents the fraction of unbroken bonds at time t_m and the function is defined as:

$$H(t_m) = \sum_{n=m}^{\infty} N(t_{n+1}) \Big/ \sum_{n=1}^{\infty} N(t_n), \text{ with } H(0) = 1 \quad (6)$$

where $N(t_n)$ is the number of bonds that break after n time steps (Haughney et al., 1987). A bond would be treated as a new one if it breaks and then re-forms. The mean lifetime of a bond is defined as:

$$\tau = \sum_{n=0}^{\infty} \frac{1}{2}\Delta t[H(t_n) + H(t_{n+1})] \quad (7)$$

where Δt is the time step (Haughney et al., 1987).

3. RESULTS

3.1. Diffusion coefficients of Mg, Si, and O in Mg_2SiO_4 liquid

To benchmark our method, the MSD of Mg, Si, and O in Mg_2SiO_4 liquids were calculated using ABACUS at different temperatures (2300 K, 3000 K, and 4000 K). In the calculations, the masses of Mg, Si, O elements were set to be 24, 28, and 16 g/mol, respectively. Fig. 1 depicts the MSD of Mg, Si, and O atoms in Mg_2SiO_4 liquid at 3000 K and Fig. 2 compares the MSD of these three species in Mg_2SiO_4 liquid at 2300 K, 3000 K, and 4000 K. Self-diffusion coefficients are fitted from the linear diffusive regimes of MSD of different temperatures, and the results are shown in Table 1. To determine the error bars, we took every 20,000 FPMD steps as a time segment and calculated diffusion coefficients in each segment using Eq. (3) for Mg, O, and Si at 2300 K. According to the Langevin equation, for most MD simulations at high temperature and low pressure, the MSD will have a ballistic regime in the short time limit (before collisions), where atoms have a straight line motion. After diffusing a distance comparable to their radius, the MSD of atoms starts the linear regime, where atoms randomly move due to collisions. The two regions are clearly shown in Figs. 1 and 2 of this as well as previous studies (e.g. Ghosh and Karki, 2011). For Mg_2SiO_4, $t < 100$ fs is the ballistic regime, where MSD is $\sim t^2$, whereas in the linear diffusive regime ($t > 1000$ fs), MSD is $\sim t$. In these two regimes, there is an intermediate part where the MSD tends to be flat because the atoms are temporarily trapped by the surrounding atoms. The intermediate regime

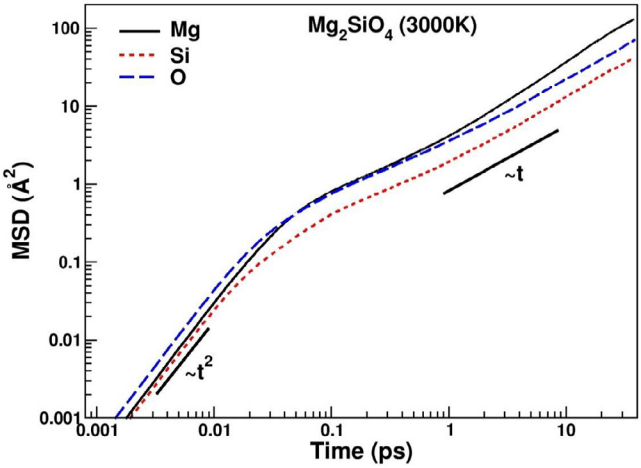

Fig. 1. Mean square displacement (MSD) of Mg (black solid line), Si (red short dash line), O (blue long dash line) species in Mg_2SiO_4 liquid as a function of time at 3000 K and 0 GPa. Two regions in the MSD are marked by bold black lines, and t^2 and t represent the ballistic regime and linear regime, respectively. (For interpretation of the references to colour in this figure legend, the reader is referred to the web version of this article.)

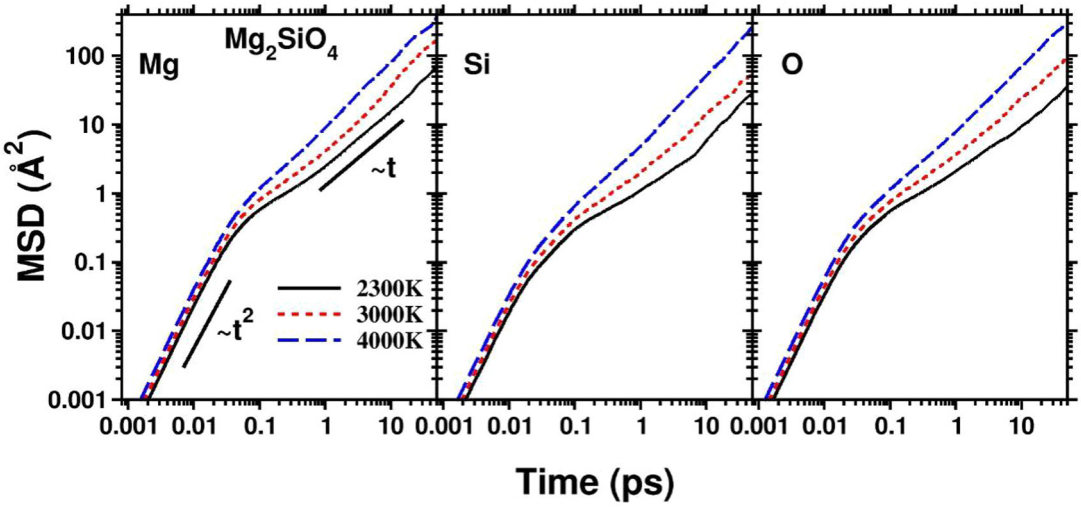

Fig. 2. MSD of different species in Mg_2SiO_4 liquid at 2300 K (black solid line), 3000 K (red short dash line), 4000 K (blue long dash line) and 0 GPa, as a function of time. Two regions in the MSD are marked by bold black lines (just shown in left panel, Si and O are the same). (For interpretation of the references to colour in this figure legend, the reader is referred to the web version of this article.)

Table 1
Diffusion coefficients of ^{24}Mg, ^{28}Si, and ^{16}O in Mg_2SiO_4 liquid at 2300 K, 3000 K, 4000 K and 0 GPa.

Diffusion coefficients (10^{-9} m^2/s)	2300 K	3000 K	4000 K
D_{Mg}	2.324 ± 0.411	5.907 ± 0.560	14.555 ± 1.058
D_{Si}	0.840 ± 0.099	2.248 ± 0.268	7.544 ± 1.570
D_O	1.277 ± 0.091	3.902 ± 0.358	10.822 ± 1.472

Note: The error was estimated from the standard deviation of the mean values of diffusion coefficients in each time segment.

is particularly evident as liquid is compressed (Ghosh and Karki, 2011). The diffusion coefficients should be fitted from the linear diffusive regime.

As we can see, the diffusion of Mg, Si, and O slows down with the decrease of the temperature. In Mg_2SiO_4 melt, Mg atoms diffuse much faster than O and Si atoms and the diffusion coefficient of Mg is about 1.5-fold of O and 2.6-fold of Si. These results are in good agreement with previous FPMD studies of the Mg_2SiO_4 system (Ghosh and Karki, 2011).

3.2. Diffusion coefficients of Mg isotopes in $MgSiO_3$ liquid

The isotope fractionation by diffusion in silicate melts has been explored using the empirical force field MD (Goel et al., 2012). The simulations were carried out in a large $MgSiO_3$ cell (containing 2160 atoms) at 4000 K and 4500 K for about 200 ns. The calculated β for Mg isotopes is 0.135 ± 0.008 at 1 atm, which has no resolvable dependence on temperature at atmospheric pressure.

We first examine the isotope effects on the Mg diffusion coefficients in $MgSiO_3$ at 4000 K. We carry out FPMD simulations using different Mg pseudo-masses, $M^* = 1$, 6, 24, 48, and 120 g/mol. The diffusion coefficients with error bars are shown in Fig. 3(a). To determine the error bars, we took every 10,000 FPMD steps as a time segment and calculated diffusion coefficients in each segment using Eq. (3). The standard deviation of the mean value was taken as the error estimation. The lighter isotopes have larger error bars than the heavier isotopes. The relationship between the Mg isotope diffusivity and the pseudo-mass can be well fitted using Eq. (1). This can be more clearly seen from Fig. 3(b), where we plot $\ln(D^{24}/D^*)$ as a function of $\ln(M^*/M^{24})$. The Mg pseudo-masses (M^*) are set as 1, 6, 24, 48, and 120 g/mol, and D^* represents the diffusion coefficients of Mg isotopes with pseudo-masses.

The results are located almost in a straight line, suggesting that the pseudo-mass approach is reliable to calculate β. The calculated value of β for Mg isotopes in $MgSiO_3$ melt is 0.272 ± 0.005 at 4000 K.

3.3. Diffusion coefficients of Mg isotopes in Mg_2SiO_4 liquid

We now study the diffusion coefficients of Mg isotopes in Mg_2SiO_4 melt. We still take the pseudo-masses of Mg isotopes as 1, 6, 24, 48, and 120 g/mol. The calculated diffusion coefficients for these pseudo-isotopes are shown in Table 2 and the diffusion coefficients with error bars are also plotted in Fig. 4(a)–(c) for T = 2300 K, 3000 K, and 4000 K, respectively. The diffusion coefficients increase dramatically with the increasing temperature because the atoms have higher kinetic energies. For example, for ^{24}Mg, the calculated diffusion coefficients are 2.324×10^{-9} m^2/s, 5.907×10^{-9} m^2/s, and 1.456×10^{-8} m^2/s at 2300 K, 3000 K, and 4000 K, respectively. Interestingly, there are notable differences in the diffusion coefficients of ^{24}Mg in Mg_2SiO_4 and in $MgSiO_3$ melts at a given temperature. For example, at 4000 K, the diffusion coefficient of ^{24}Mg is 1.456×10^{-8} m^2/s in Mg_2SiO_4 liquid, compared to 1.921×10^{-8} m^2/s in $MgSiO_3$ liquid as listed in Table 3. On the other hand, Si and O have similar diffusion coefficients in the two liquids.

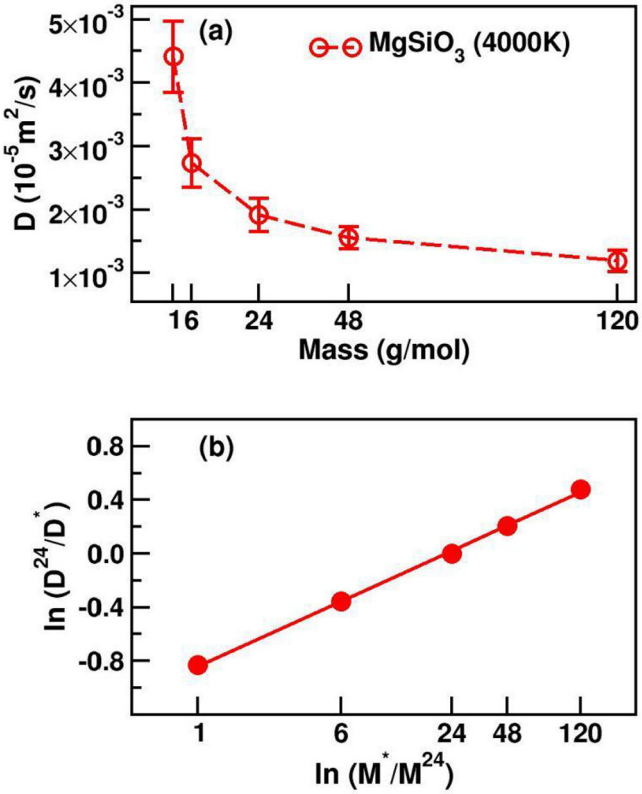

Fig. 3. (a) Diffusion coefficients with error bars for Mg isotopes in $MgSiO_3$ liquid, as a function of isotope pseudo-mass at 4000 K and 0 GPa; (b) $\ln(D^{24}/D^*)$ as a function of $\ln(M^*/M^{24})$ in $MgSiO_3$ liquid at 4000 K and 0 GPa. The Mg pseudo-masses are taken to be $M^* = 1$, 6, 24, 48, and 120 g/mol, and D^* represents the diffusion coefficient of pseudo-masses Mg isotopes. For $MgSiO_3$ melt, β is 0.272 ± 0.005 at 4000 K and 0 GPa.

Table 2
Diffusion coefficients of Mg isotopes in Mg_2SiO_4 liquid at 2300 K, 3000 K, 4000 K and 0 GPa.

Diffusion coefficients (10^{-9} m^2/s)	2300 K	3000 K	4000 K
D^1_{Mg}	4.270 ± 0.563	12.906 ± 1.275	30.726 ± 1.442
D^6_{Mg}	3.056 ± 0.443	8.697 ± 0.937	19.478 ± 1.308
D^{24}_{Mg}	2.324 ± 0.411	5.907 ± 0.560	14.555 ± 1.058
D^{48}_{Mg}	2.070 ± 0.485	4.920 ± 0.960	11.105 ± 0.646
D^{120}_{Mg}	1.362 ± 0.238	4.097 ± 0.515	8.939 ± 0.972

Note: The error was estimated from the standard deviation of the mean values of diffusion coefficients in each time segment.

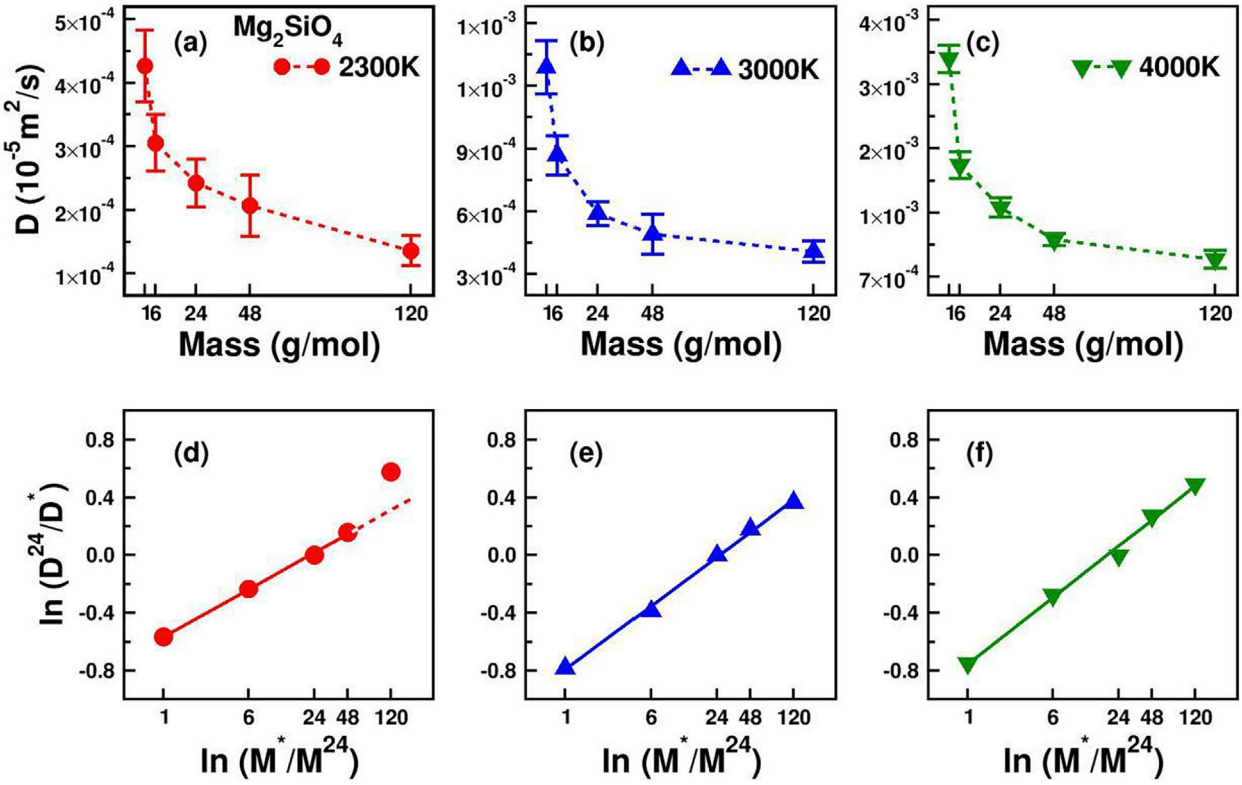

Fig. 4. (a)–(c) Diffusion coefficients with error bars of Mg isotopes in Mg_2SiO_4 liquid, as a function of isotope mass at 2300 K, 3000 K, 4000 K and 0 GPa; (d), (e), (f) $\ln(D^{24}/D^*)$, as a function of $\ln(M^*/M^{24})$ in Mg_2SiO_4 liquid at 2300 K, 3000 K, 4000 K and 0 GPa. The straight line in (d) was fitted using the data of $M^* = 1$, 6, 24, and 48 g/mol. The straight lines in (e) and (f) were fitted using the data of $M^* = 1$, 6, 24, 48 and 120 g/mol, and D^* represents the diffusion coefficient of pseudo-masses Mg isotopes. For Mg_2SiO_4 melt, β is 0.184 ± 0.006 at 2300 K, 0.245 ± 0.007 at 3000 K, and 0.257 ± 0.012 at 4000 K.

Table 3
Diffusion coefficients of isotope ^{24}Mg, ^{28}Si, and ^{16}O species in $MgSiO_3$ and Mg_2SiO_4 liquids at 4000 K, 0 GPa.

	D_{Mg} (10^{-8} m^2/s)	D_{Si} (10^{-8} m^2/s)	D_O (10^{-8} m^2/s)	D_{Mg}/D_{Si}	β
Mg_2SiO_4	1.456 ± 0.106	0.754 ± 0.157	1.082 ± 0.147	1.931	0.257 ± 0.012
$MgSiO_3$	1.921 ± 0.260	0.895 ± 0.082	1.196 ± 0.163	2.146	0.272 ± 0.005

Note: The error was estimated from the standard deviation of the mean values of diffusion coefficients in each time segment.

We plot $\ln(D^{24}/D^*)$ vs. $\ln(M^*/M^{24})$ of Mg_2SiO_4 liquid in Fig. 4(d)–(f), for T = 2300 K, 3000 K, and 4000 K, respectively. The diffusion coefficients of Mg isotopes in Mg_2SiO_4 liquid fall on straight lines in these figures, except the data of $M^* = 120$ g/mol at 2300 K, which significantly deviates from the straight line. This result will be explained in Section 4.3.

For Mg_2SiO_4 liquid, the fitted β value of Mg isotopes is 0.184 ± 0.006 at 2300 K, 0.245 ± 0.007 at 3000 K, and 0.257 ± 0.012 at 4000 K, where the errors of β come from

linear fitting of calculated data. The results suggest that β values are relatively insensitive to the temperature when it is far above the liquidus. This notion is consistent with the results of Goel et al. (2012). However, the β values may be quite different at temperatures that are close to the melting point at about 2300 K.

4. DISCUSSION

4.1. Accuracy of FPMD calculation

In this study, we carried out FPMD simulations on silicate melts at different temperatures. MSD and diffusion coefficients were calculated by sampling the simulation trajectories. To make sure that simulations were sampling the equilibrium trajectories, we calculated the EOS of melt Mg_2SiO_4 at 2300 K and theoretical parameters (volume V_0, bulk modulus K_0 and its first pressure derivative K_0') were obtained by fitting the Birch (1947) EOS (Eq. (2)) based on pressure versus volume curves from our FPMD simulations. Pressures were calculated under different volumes: $0.5V_x$, $0.6V_x$, $0.75V_x$, $0.8V_x$, $0.9V_x$ and $1.0V_x$ (V_x = 52.36 cm^3/mol). In the canonical ensemble, instantaneous values of pressure have no thermodynamic meaning, therefore average pressures have been calculated from different time steps. The data on volumes (or box densities) used and average pressure values obtained are given in Table 4.

The comparison of our theoretical values at 2300 K with those from recent experimental and FPMD studies at the ambient melting point (2163 K) is given in Table 5. The calculated volume V_0 and K_0' are in excellent agreement with the experimental values in Table 5. The experimental bulk modulus K_0 has a wide range of values. Our results fall into this range and are also close to the previous FPMD results in de Koker et al. (2008). The good agreement of our results with those from recent studies indicates that our sampling is from equilibrium trajectories at 2300 K, so is the case at 3000 K and 4000 K because it is easier to reach equilibrium or steady state at higher temperatures.

In Tables 1–3, diffusion coefficients were calculated using Eq. (3), which is only appropriate for "long time" simulations. Therefore, sufficient sampling of equilibrium trajectories is an additional requirement for accurate estimation of diffusion coefficients. For this purpose, we prolonged our simulation of ^{24}Mg isotope in Mg_2SiO_4 system at 2300 K up to 90 ps. Using 20 ps trajectories with averaging over 5000 initial configurations, we have totally 15 time segments: 0–20, 5–25, 10–30, …, 70–90. The average diffusion coefficients and their standard deviations are obtained from these time segments. The calculated diffusion coefficients of Mg, Si, and O elements are 2.319 ± 0.342, 0.767 ± 0.172, and 1.243 ± 0.117 (10^{-9} m^2/s), respectively. We note that the standard deviations maybe underestimated because of the overlap between the time segments, which is a compromise for the short simulation time. These results from "long time" simulation (90 ps) are same within the error with those from simulations with 60 ps in Table 1, which indicates that simulation time of 60 ps is long enough to obtain reliable diffusion coefficients.

Table 5
Comparison of equation of state between FPMD and experimental data.

	FPMD 2163 K	Experiment	This study 2300 K
V_0 (cm^3/mol)	53.55[a]	53.5[b] 52.4[c] 9.5[c]	53.87
K_0 (GPa)	23[a]	24.3[d] 27[e] 59[f]	33.69
K_0'	7[a]	3.75[f] 6.9 [g]	5.55

[a] de Koker et al. (2008).
[b] Lange (1997).
[c] Lange and Carmichael (1987).
[d] Ai and Lange (2008).
[e] Rivers and Carmichael (1987).
[f] Bottinga (1985).
[g] Rigden et al. (1989).

4.2. Diffusion process in silicate liquids

As shown in the ballistic regime in Fig. 1, the lighter oxygen atoms move faster than Mg and Si. However, in the linear diffusive regime, Mg atoms diffuse much faster than O atoms which are further faster than Si atoms in Mg_2SiO_4 liquid system. To understand these results, we need to take account of the position of atoms in the silicate melts. Si atoms are in the center of Si—O tetrahedron which has strong chemical bonds between Si and O atoms even in liquids. To show this, we plot the Si—O partial radial distribution functions $g_{Si\text{-}O}(r)$ in Mg_2SiO_4 liquids at 2300 K, 3000 K, and 4000 K in Fig. 5(a). The mass of the Mg isotope is 24 g/mol. The Si—O pair distribution functions $g_{Si\text{-}O}(r)$ show very sharp peaks, indicating strong Si—O bonds in the liquids. With the increasing temperature, $g_{Si\text{-}O}(r)$ becomes more extended, accompanied by the lowering of the peaks. However, even at 4000 K, the peaks are still

Table 4
Pressures under different volumes (or box densities) of melt Mg_2SiO_4 at 2300 K, where V_x = 52.36 cm^3/mol is the reference volume.

	Volume (10^{-30} cm^3)	Density (g/cm^3)	Pressure (GPa)
$0.5V_x$	1394.203	5.338	178.460
$0.6V_x$	1673.002	4.448	81.757
$0.75V_x$	2091.251	3.559	23.481
$0.8V_x$	2230.671	3.336	17.648
$0.9V_x$	2509.500	2.965	7.322
$1.0V_x$	2788.337	2.669	0.993

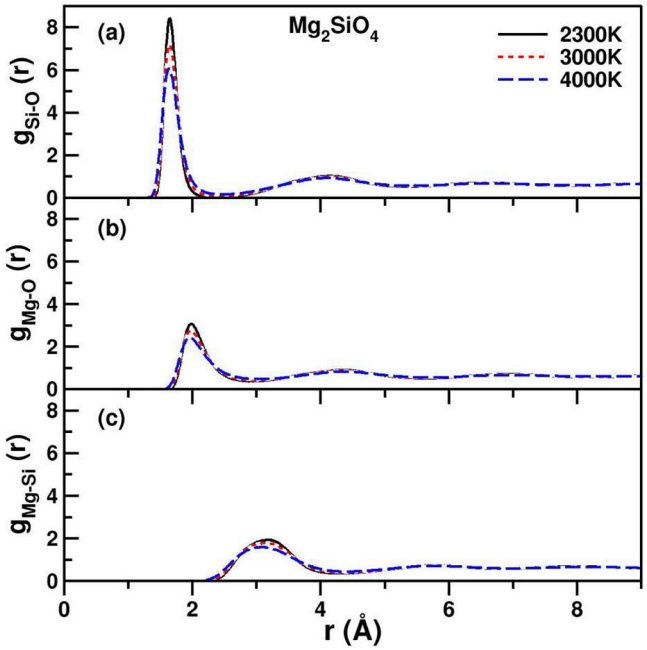

Fig. 5. Radial distribution functions g(r) for Si—O pair(a), Mg—O pair(b), and Mg—Si pair(c) in Mg_2SiO_4 liquid with ^{24}Mg isotope at 2300 K (black solid line), 3000 K (red short dash line), 4000 K (blue long dash line) and 0 Gpa. $g_{\alpha\text{-}\beta}$ gives the density probability for an atom of the α species with a neighbor of the β species at a given distance r. (For interpretation of the references to colour in this figure legend, the reader is referred to the web version of this article.)

sharp and strong. We also plot the bonds decay functions H (t) of Si—O bonds in Fig. 6(a) at the three temperatures. The results show that, at 3000 K, about 20% Si—O bonds are intact after 1.2 ps (1200 time steps). Even at temperature up to 4000 K, 20% Si—O bonds are still intact after 0.7 ps, which indicates the Si—O bonds are stable.

To compare with the Si—O pair, we also plot the pair distribution functions for Mg—O pair $g_{Mg\text{-}O}(r)$ in Fig. 5 (b) and Mg—Si pair $g_{Mg\text{-}Si}(r)$ in Fig. 5(c). Both Mg—O and Mg—Si have much larger bond lengths than Si—O. $g_{Mg\text{-}O}(r)$ and $g_{Mg\text{-}Si}(r)$ also show much weaker and broader peaks than $g_{Si\text{-}O}(r)$. These results are consistent with the fact that Mg atoms are network modifier cations which form bonds with O^{2-} weaker than Si—O bonds (Fig. 5). Therefore, Mg atoms can move relatively easily in available open spaces (Ghosh and Karki, 2011).

In Fig. 6(b) and (c), to compare with the strongly bonded Si—O pair, we plot the bond decay function H(t) as a function of time for Mg—O and Mg—Si pairs. For these two bonds, H(t) decays much more rapidly than Si—O pair, and the mean bond life-times of Mg—O bonds and Mg—Si bonds are much shorter than those of Si—O bonds, as shown in Table 6. These indicate that Mg—O and Mg—Si bonds break more easily than Si—O bond, which is another reason why Mg atoms move much faster than O and Si atoms in Mg_2SiO_4 liquids.

4.3. Composition and temperature effects on diffusion coefficients of isotopes

The composition effect on diffusive process is important for better understanding kinetic isotope fractionation. For Mg_2SiO_4 liquid at 4000 K, the β value for Mg isotopes is 0.257 ± 0.012, which is slightly lower than β (0.272 ± 0.005) for Mg isotopes in $MgSiO_3$ liquid within errors. Watkins et al. (2011) show large dependence of β values of Ca isotopes on $SiO_2 - Al_2O_3$ contents in liquids, suggesting that higher values of β tend to occur in liquids with higher $SiO_2 + Al_2O_3$ contents. This was explained as follows: the mass discrimination caused by isotope diffusion is related to the solute-solvent interactions in silicate melts, and β factors vary systematically with the solvent-normalized diffusivity, i.e., $\beta \sim D_X/D_{Si}$ ratio (Watkins et al., 2011, 2017), which means that the strong coupling of cation of interest to the silicate network can reduce the diffusivity and β value in silicate melts. As listed in Table 3 and Fig. 7a, the D_{Mg}/D_{Si} ratio (1.931) of Mg_2SiO_4 is lower than that of $MgSiO_3$ (2.146), and β for Mg_2SiO_4 is smaller than for $MgSiO_3$, consistent with the solvent-normalized diffusivity.

Even though the isotope diffusion coefficients increase dramatically with the increasing temperature, the mass dependence of Mg isotope diffusion, namely β, does not appear to be sensitive to the variation of temperature when it is well above liquidus of Mg_2SiO_4 (2163 K). For Mg_2SiO_4, β is 0.245 at 3000 K, close to β value (0.257) at 4000 K. However, at 2300 K, which is close to the liquidus temperature (2163 K), the β is 0.184, which is significantly smaller than those of higher temperatures. Especially, we find that the calculated $\ln(D^{24}/D^*)$ for $M^* = 120$ g/mol at 2300 K significantly deviates from the straight line in Fig. 4(d). This deviation may due to the extremely large $M^* = 120$ g/mol. From a simple argument by Lindemann's criterion, a system with larger atomic mass will have a

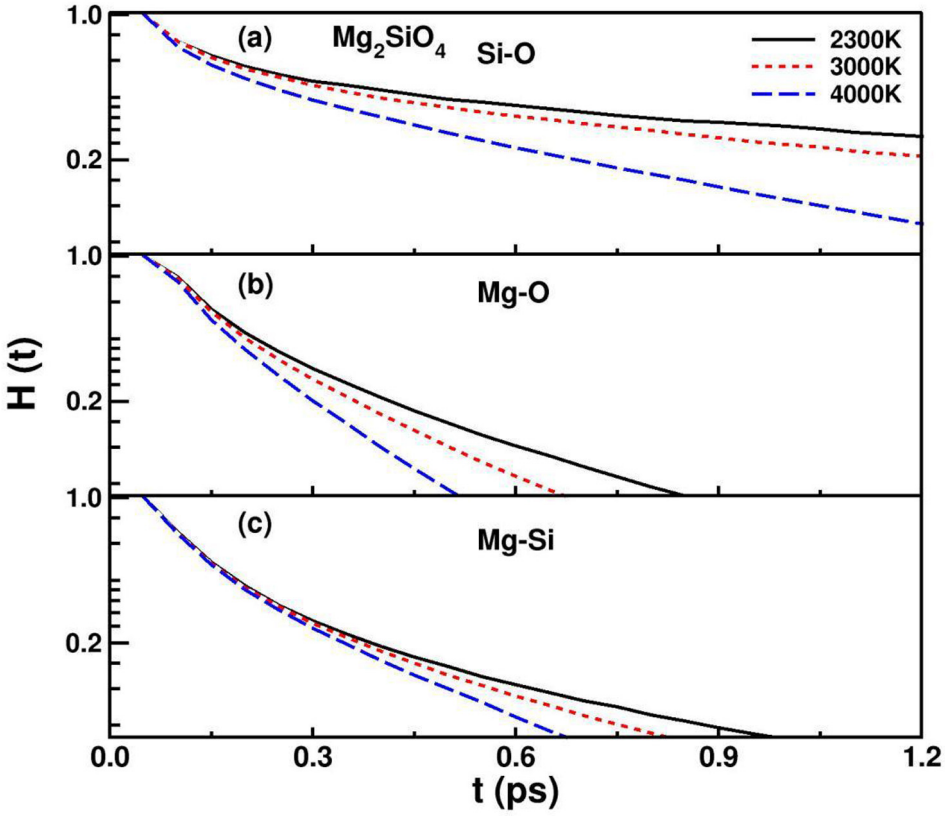

Fig. 6. Bond decay functions H(t) for for Si—O pair(a), Mg—O pair(b) and Mg—Si pair(c) in Mg_2SiO_4 liquid with ^{24}Mg isotope at 2300 K (black solid line), 3000 K (red short dash line), 4000 K (blue long dash line) and 0 GPa. (For interpretation of the references to colour in this figure legend, the reader is referred to the web version of this article.)

Table 6
Mean lifetime of bonds between different atom species (Mg, Si and O) in Mg_2SiO_4 liquid at 2300 K, 3000 K, 4000 K and 0 GPa.

τ (ps)	2300 K	3000 K	4000 K
τ_{Si-O}	0.98	0.74	0.40
τ_{Mg-O}	0.26	0.21	0.17
τ_{Mg-Si}	0.27	0.23	0.19

higher melting point (Lindemann, 1910). Therefore, if $M^* =$ 120 g/mol is used, the melting point will increase. Therefore, the relation Eq. (1) may result in large uncertainty at this point. We therefore dropped this data point in fitting β.

We noticed that β increases while D_{Mg}/D_{Si} decreases with temperature increasing in Mg_2SiO_4 melt (Fig. 7a), which may be related to the effect of melt structure with temperature change. The distributions of g(r) and H(t) indicate that chemical bonds in Mg_2SiO_4 melt are weaker and are more easily broken under higher temperature. Therefore, Mg and Si both diffuse more freely, and the diffusivities of Mg and Si atoms exhibit smaller difference at higher temperature. Even though D_{Mg}/D_{Si} is smaller under higher temperature, Mg isotope diffusion shows larger mass discrimination because Mg isotopes diffuse faster and more freely under this condition. This also indicates that the solvent-normalized diffusivity D_x/D_{Si} (x represents the species of interest) is not the only parameter to determine β. β and D_x/D_{Si} are both related to the degree of coupling between species x and solvent (represented by Si) (Goel et al., 2012). Because the silicate networks are more likely broken at high temperatures, both species x and Si will diffuse more freely and faster, resulting in smaller D_x/D_{Si} and larger diffusive mass discrimination of isotopes of species x.

4.4. Comparison with previous experimental and theoretical studies

The diffusion couple experiments of Richter et al. (2008) and Watkins et al. (2011) showed that β factor of Mg isotopes was about 0.050 ± 0.005 in basalt-rhyolite silicate liquids at 1400 °C and 1 GPa, and 0.100 ± 0.010 in albite-diopside liquids at 1450 °C and 8 kbar. The β factors of Mg from FPMD simulations at 0 GPa are 0.184 ± 0.006 at 2300 K, 0.245 ± 0.007 at 3000 K, 0.257 ± 0.012 at 4000 K in Mg_2SiO_4 liquid, and 0.272 ± 0.005 at 4000 K in $MgSiO_3$ liquid, much higher than the experimental data. The simulations in this study were all conducted under 0 GPa, lower than the pressure of laboratory experiments (~1 GPa). MD simulations of Goel et al. (2012) show that β value for Mg in $MgSiO_3$ melt is 0.135 ± 0.008 at 0 GPa, 0.092 ± 0.006 at 25 GPa and 0.084 ± 0.016 at 50 GPa, indicating that β decreases with pressure increasing. However,

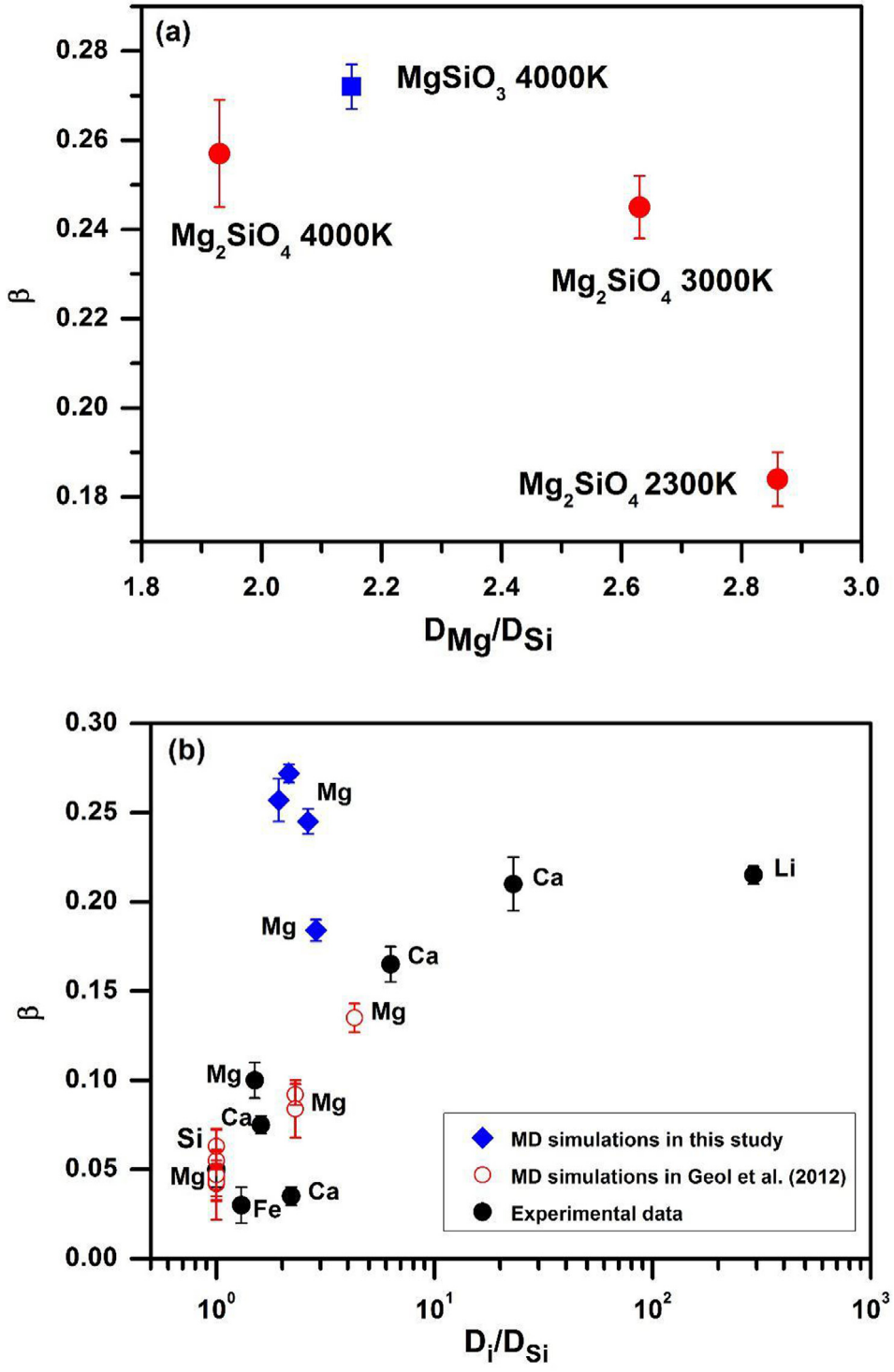

Fig. 7. (a) Correlation between the mass dependence of isotope diffusion factor (β) and solvent-normalized diffusivity (D_{Mg}/D_{Si}) with both temperature and composition changes in Mg_2SiO_4 and $MgSiO_3$ melts. (b) The β factors correlate with D_i/D_{Si} (i represents cation) in silicate melts. Experimental data are from Richter et al. (2003, 2008, 2009b) and Watkins et al. (2011). MD simulations data are from Goel et al. (2012).

the small difference of pressure (~1 GPa) cannot result in such significant difference of β between experiments and FPMD calculations. Note that our simulations were performed at much higher temperatures (2300 K, 3000 K, and 4000 K) compared to the diffusion experiments performed at about 1400 °C (Richter et al., 2008; Watkins et al., 2011). Because Mg diffuses faster and Mg isotopes exhibit more mass discrimination at higher temperatures,

the large temperature difference may contribute to significant difference of β between experimental studies and FPMD calculations.

Finally, we simulated ideal silicate melts only including Mg, Si, and O element, a simplified case relative to the complex natural melt in experimental studies. Watkins et al. (2011) shows that β can be highly variable for a given cation depending on melt composition. In experimental studies, there are many other major elements, which could form complex chemical bonds with the Mg ions (such as Al), and therefore affect the diffusion process in the melts. As shown in Fig. 7b, β values for Mg isotopes and D_{Mg}/D_{Si} of our FPMD results are significantly higher than these two experimental values, indicating that weaker interactions between Mg and melt matrix always produce higher β values (Watkins et al., 2017). It would be interesting to examine how the additional species change the isotope effects of Mg in future FPMD studies. Overall, the disparity of β between experimental studies and FPMD calculations is mainly due to the large temperature and chemical composition differences.

Goel et al. (2012) reported the $\beta = 0.135 \pm 0.008$ for Mg isotopes in $MgSiO_3$ at 4000 K from empirical force field simulations, compared to $\beta = 0.272 \pm 0.005$ from our FPMD simulations. The significant difference between the two values probably originates from the different methods used to deal with the atomic interactions. During the diffusion process, the chemical environment surrounding atoms keeps changing all the time, especially at high temperature there are large amount of chemical bonding and bond breaking. For example, as shown in Fig. 5(a)–(c), Mg and O atoms may pair up and form weak chemical bonds, but the bonds break easily and quickly. Compared to the classical MD based on empirical potentials, FPMD can describe this process more accurately, especially in the complex materials (Lundqvist and March, 1983). The interaction potentials used in FPMD simulations are more accurate than those in classical MD. However FPMD simulations are significantly computationally more demanding, and are limited to small cell size and short simulation time compared to classical MD simulations which may result in additional errors.

4.5. Future perspectives

Diffusion is the fundamental process for mass transfer in the terrestrial planets which can produce large isotope fractionation even at high temperatures. Knowing isotope diffusion coefficients in melts is critical to study diffusive isotope fractionation which can provide valuable information on relevant geochemical processes and timescales. FPMD calculation provides a novel and promising method to theoretically calculate isotope diffusion coefficients in compositionally complicated nature melts.

β factors of stable isotopes in complicated silicate melts are controlled by species of elements which are further related to temperature and pressure. Currently, the applications of FPMD calculation in kinetic isotope fractionation are mainly constrained by computing resource. Fig. 8 shows that, for Mg_2SiO_4 system at 3000 K, calculation time increases with the cell size growing in a given number of cores (Fig. 8(a)), and the time reduces if the number of cores increases in a given cell size (Fig. 8(b)). In this study, we chose the cell size with 224 atoms for Mg_2SiO_4 and it took about two months for each isotope FPMD calculation at a given temperature with 48 cores. Therefore, it is still challenging to study the real, complex systems. Lower temperatures and higher pressures require longer simulation time to achieve equilibrium. More chemically complex compositions and water-containing systems need even larger

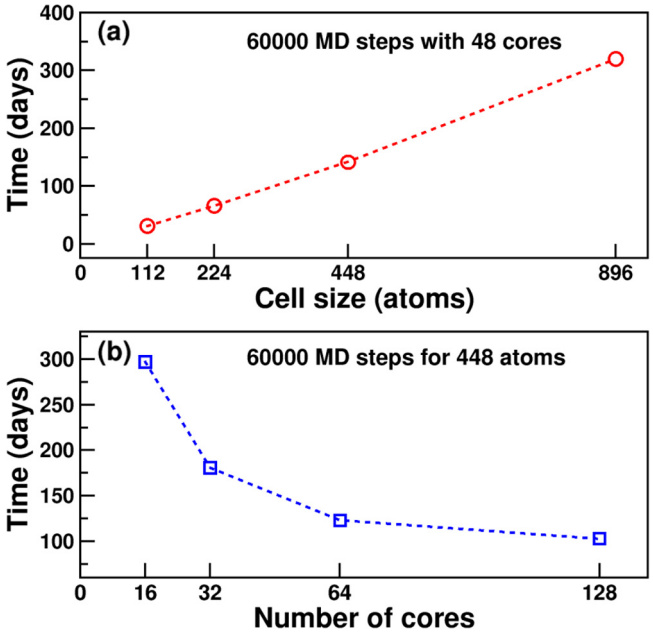

Fig. 8. Estimated calculation time of (a) different sizes of Mg_2SiO_4 systems at 3000 K for 60,000 FPMD steps with 48 cores and (b) Mg_2SiO_4 system with 448 atoms at 3000 K for 60,000 FPMD steps with different number of cores.

systems to simulate, which needs significantly more computational resources.

With the fast development of high-performance supercomputer in the future, we will be able to simulate more complex systems with composition and temperature close to the natural magmatic systems. This method will be helpful for us to understand the mechanisms of diffusion-driven kinetic isotope fractionation. Especially, FPMD can calculate β factors for isotopes of trace elements in silicates melt, such as Cu, Zn, Cr, Mo, and V, which are absent of experimental and MD studies. Furthermore, FPMD may be used to study isotope mass dependence of diffusion in evolving magma which is recorded in minerals. For example, large Fe and Mg isotope fractionation caused by inter-diffusion of Mg and Fe between olivines and evolving melts can be used to calculate the cooling rate of Kilauea Iki lava lake (Teng et al., 2011). If we can obtain accurate Mg and Fe isotope diffusion coefficients in natural silicate melts and minerals, the cooling rate of lave lake can be better constrained.

5. CONCLUSIONS

This study presents first-principle MD simulations to calculate the β factors of Mg isotope diffusion in silicate melts. We used pseudo-isotope method assuming that Mg isotopes have atomic mass of 1, 6, 24, 48, and 120 g/mol to estimate β for $MgSiO_3$ and Mg_2SiO_4 melts. The calculated β value of Mg isotopes is 0.272 ± 0.005 in $MgSiO_3$ liquid at 4000 K. For Mg_2SiO_4 liquid, the calculated β values are: 0.184 ± 0.006 at 2300 K, 0.245 ± 0.007 at 3000 K, and 0.257 ± 0.012 at 4000 K. Therefore, β values are not very sensitive to the temperature if it is well above the liquidus, but can be significantly smaller when close to the liquidus. The small difference of β between simple silicate liquids with compositions of $MgSiO_3$ and Mg_2SiO_4 suggests that the β value may depend on the chemical composition of the melts. Future work could investigate the β values in more complex silicate liquids which are close to the natural silicate melts with the development of high-performance supercomputer.

ACKNOWLEDGMENTS

This work is supported by the Strategic Priority Research Program (B) of Chinese Academy of Sciences (Grant No. XDB18000000), the National Science Foundation of China (41325011, 41630206, and 11374275), and the National Key Research and Development Program of China (Grants No. 2016YFB0201202). The numerical calculations have been done on the USTC HPC facilities. We are grateful to Frédéric Moynier for the comments and editorial handling. We also thank three anonymous reviewers for the constructive comments.

REFERENCES

Ai Y. and Lange R. A. (2008) The compressibility of CaO–MgO–Al_2O_3–SiO_2 liquids from new acoustic velocity measurements: reevaluation of the equation of state of $CaMgSi_2O_6$–$CaAl_2SiO_8$ liquids to 25 GPa. *J. Geophys. Res.* **113**, B04203.

Beck P., Chaussidon M., Barrat J. A., Gillet P. and Bohn M. (2006) Diffusion induced Li isotopic fractionation during the cooling of magmatic rocks: the case of pyroxene phenocrysts from nakhlite meteorites. *Geochim. Cosmochim. Acta* **70**(18), 4813–4825.

Bigeleisen J. and Mayer M. G. (1947) Calculation of equilibrium constants for isotopic exchange reactions. *J. Chem. Phys.* **15**(5), 261–267.

Birch F. (1947) Finite elastic strain of cubic crystals. *Phys. Rev.* **71** (11), 809.

Bottinga Y. (1985) On the isothermal compressibility of silicate liquids at high pressure. *Earth Planet. Sci. Lett.* **74**(4), 350–360.

Bourg I. C. and Sposito G. (2007) Molecular dynamics simulations of kinetic isotope fractionation during the diffusion of ionic species in liquid water. *Geochim. Cosmochim. Acta* **71**(23), 5583–5589.

Bourg I. C. and Sposito G. (2008) Isotopic fractionation of noble gases by diffusion in liquid water: molecular dynamics simulations and hydrologic applications. *Geochim. Cosmochim. Acta* **72**(9), 2237–2247.

Bourg I. C., Richter F. M., Christensen J. N. and Sposito G. (2010) Isotopic mass dependence of metal cation diffusion coefficients in liquid water. *Geochim. Cosmochim. Acta* **74**(8), 2249–2256.

Bowen N. L. and Andersen O. (1914) The binary system MgO-SiO_2. *Am. J. Sci.* **222**, 487–500.

Chen M., Guo G. and He L. (2010) Systematically improvable optimized atomic basis sets for ab initio calculations. *J. Phys. Condens. Matter* **22**(44), 445501.

Chen M., Guo G. and He L. (2011) Electronic structure interpolation via atomic orbitals. *J. Phys. Condens. Matter* **23**(32), 325501.

Chopra R., Richter F. M., Watson E. B. and Scullard C. R. (2012) Magnesium isotope fractionation by chemical diffusion in natural settings and in laboratory analogues. *Geochim. Cosmochim. Acta* **88**, 1–18.

Dauphas N. (2007) Diffusion-driven kinetic isotope effect of Fe and Ni during formation of the Widmanstätten pattern. *Meteoritics. Planet. Sci.* **42**(9), 1597–1613.

Dauphas N., Teng F.-Z. and Arndt N. T. (2010) Magnesium and iron isotopes in 2.7 Ga Alexo komatiites: mantle signatures, no evidence for Soret diffusion, and identification of diffusive transport in zoned olivine. *Geochim. Cosmochim. Acta* **74**(11), 3274–3291.

de Koker N. P., Stixrude L. and Karki B. B. (2008) Thermodynamics, structure, dynamics, and freezing of Mg_2SiO_4 liquid at high pressure. *Geochim. Cosmochim. Acta* **72**, 1427–1441.

Einstein A. (1956) Investigations on the Theory of the Brownian Movement. Courier Corporation.

Gausonne N., Schmitt A. D., Heuser A., Wombacher F., Dietzel M., Tipper E. and Schiller M. (2016) *Calcium Stable Isotope Geochemistry*. Springer, Berlin.

Ghosh D. B. and Karki B. B. (2011) Diffusion and viscosity of Mg_2SiO_4 liquid at high pressure from first-principles simulations. *Geochim. Cosmochim. Acta* **75**(16), 4591–4600.

Giannozzi P., Baroni S., Bonini N., Calandra M., Car R., Cavazzoni C., Ceresoli D., Chiarotti G. L., Cococcioni M., Dabo I., Dal Corso A., De Gironcoli S., Fabris S., Fratesi G., Gebauer R., Gerstmann U., Gougoussis C., Kokalj A., Lazzeri M., Martin-Samos L., Marzari N., Mauri F., Mazzarello R., Paolini S., Pasquarello A., Paulatto L., Sbraccia C., Scandolo S., Sclauzero G., Seitsonen A. P., Smogunov A., Umari P. and Wentzcovitch R. M. (2009) QUANTUM ESPRESSO: a modular and open-source software project for quantum simulations of materials. *J. Phys. Condens. Matter* **21**(39), 395502.

Goel G., Zhang L., Lacks D. J. and Van Orman J. A. (2012) Isotope fractionation by diffusion in silicate melts: insights from

molecular dynamics simulations. *Geochim. Cosmochim. Acta* **93**, 205–213.

Haughney M., Ferrario M. and McDonald I. R. (1987) Molecular-dynamics simulation of liquid methanol. *J. Phys. Chem.* **91**(19), 4934–4940.

Hess B., Kutzner C., Van Der Spoel D. and Lindahl E. (2008) GROMACS 4: algorithms for highly efficient, load-balanced, and scalable molecular simulation. *J. Chem. Theor. Comput.* **4** (3), 435–447.

Huang F., Lundstrom C., Glessner J., Ianno A., Boudreau A., Li J., Ferre EC., Marshak S. and DeFrates J. (2009) Chemical and isotopic fractionation of wet andesite in a temperature gradient: experiments and models suggesting a new mechanism of magma differentiation. *Geochim. Cosmochim. Acta* **73**, 729–749.

Huang F., Chakraborty P., Lundstrom C. C., Holmden C., Glessner J. J. G., Kieffer S. W. and Lesher C. E. (2010) Isotope fractionation in silicate melts by thermal diffusion. *Nature* **464** (7287), 396–400.

Knight K. B., Kita N. T., Mendybaev R. A., Richter F. M., Davis A. M. and Valley J. W. (2009) Silicon isotopic fractionation of CAI-like vacuum evaporation residues. *Geochim. Cosmochim. Acta* **73**(20), 6390–6401.

Lange R. A. and Carmichael I. S. (1987) Densities of Na_2O K_2O–CaO–MgO–Fe-Fe_2O_3-Al_2O_3-TiO_2-SiO_2 liquids: new measurements and derived partial molar properties. *Geochim. Cosmochim. Acta* **51**(11), 2931–2946.

Lange R. A. (1997) A revised model for the density and thermal expansivity of K_2O-Na_2O-CaO-MgO-Al_2O_3-SiO_2 liquids from 700 to 1900 K: extension to crustal magmatic temperatures. *Contrib. Mineral. Petrol.* **130**(1), 1–11.

Li P., Liu X., Chen M., Lin P., Ren X., Lin L., Yang C. and He L. (2016) Large-scale ab initio simulations based on systematically improvable atomic basis. *Comput. Mater. Sci.* **112**, 503–517.

Lindemann F. A. (1910) The calculation of molecular vibration frequencies. *Physik. Z* **11**, 609–612.

Lundqvist S. and March N. M. (1983) *Theory of the Inhomogeneous Electron Gas*. Plenum, New York.

Lundstrom C. C., Chaussidon M., Hsui A. T., Kelemen P. and Zimmerman M. (2005) Observations of Li isotopic variations in the Trinity Ophiolite: evidence for isotopic fractionation by diffusion during mantle melting. *Geochim. Cosmochim. Acta* **69** (3), 735–751.

Marrocchelli D., Salanne M. and Madden P. A. (2010) High-pressure behaviour of GeO_2: a simulation study. *J. Phys. Condens. Matter* **22**(15), 152102.

Oeser M., Dohmen R., Horn I., Schuth S. and Weyer S. (2015) Processes and time scales of magmatic evolution as revealed by Fe–Mg chemical and isotopic zoning in natural olivines. *Geochim. Cosmochim. Acta* **154**, 130–150.

Parkinson I. J., Hammond S. J., James R. H. and Rogers N. W. (2007) High-temperature lithium isotope fractionation: insights from lithium isotope diffusion in magmatic systems. *Earth Planet. Sci. Lett.* **257**(3), 609–621.

Plimpton S. (1995) Fast parallel algorithms for short-range molecular dynamics. *J. Comput. Phys.* **117**(1), 1–19.

Richter F. M., Liang Y. and Davis A. M. (1999) Isotope fractionation by diffusion in molten oxides. *Geochim. Cosmochim. Acta* **63**(18), 2853–2861.

Richter F. M., Davis A. M., DePaolo D. J. and Watson E. B. (2003) Isotope fractionation by chemical diffusion between molten basalt and rhyolite. *Geochim. Cosmochim. Acta* **67**(20), 3905–3923.

Richter F. M., Watson E. B., Mendybaev R. A., Teng F.-Z. and Janney P. E. (2008) Magnesium isotope fractionation in silicate melts by chemical and thermal diffusion. *Geochim. Cosmochim. Acta* **72**(1), 206–220.

Richter F. M., Dauphas N. and Teng F.-Z. (2009a) Non-traditional fractionation of non-traditional isotopes: evaporation, chemical diffusion and Soret diffusion. *Chem. Geol.* **258**(1), 92–103.

Richter F. M., Watson E. B., Mendybaev R., Dauphas N., Georg B., Watkins J. and Valley J. (2009b) Isotopic fractionation of the major elements of molten basalt by chemical and thermal diffusion. *Geochim. Cosmochim. Acta* **73**(14), 4250–4263.

Rigden S. M., Ahrens T. J. and Stolper E. M. (1989) High-pressure equation of state of molten anorthite and diopside. *J. Geophys. Res.* **94**, 9508–9522.

Rivers M. L. and Carmichael I. S. E. (1987) Ultrasonic studies of silicate melts. *J. Geophys. Res.* **92**, 9247–9270.

Rudnick R. L. and Ionov D. A. (2007) Lithium elemental and isotopic disequilibrium in minerals from peridotite xenoliths from far-east Russia: product of recent melt/fluid–rock interaction. *Earth Planet. Sci. Lett.* **256**, 278–293.

Sio C. K. I. and Dauphas N. (2017) Thermal and crystallization histories of magmatic bodies by Monte Carlo inversion of Mg-Fe isotopic profiles in olivine. *Geology* **45**(1), 67–70.

Teng F.-Z., McDonough W. F., Rudnick R. L. and Walker R. J. (2006) Diffusion-driven extreme lithium isotopic fractionation in country rocks of the Tin Mountain pegmatite. *Earth Planet. Sci. Lett.* **243**(3–4), 701–710.

Teng F.-Z., Dauphas N., Helz R. T., Gao S. and Huang S. (2011) Diffusion-driven magnesium and iron isotope fractionation in Hawaiian olivine. *Earth Planet. Sci. Lett.* **308**(3), 317–324.

Tsuchiyama A., Kawamura K., Nakao T. and Uyeda C. (1994) Isotopic effects on diffusion in MgO melt simulated by the molecular dynamics (MD) method and implications for isotopic mass fractionation in magmatic systems. *Geochim. Cosmochim. Acta* **58**(14), 3013–3021.

Urey H. C. (1947) The thermodynamic properties of isotopic substances. *J. Chem. Soc.*, 562–581.

Van Orman J. A. and Krawczynski M. J. (2015) Theoretical constraints on the isotope effect for diffusion in minerals. *Geochim. Cosmochim. Acta* **164**, 365–381.

Watkins J. M., DePaolo D. J., Huber C. and Ryerson F. J. (2009) Liquid composition-dependence of calcium isotope fractionation during diffusion in molten silicates. *Geochim. Cosmochim. Acta* **73**(24), 7341–7359.

Watkins J. M., DePaolo D. J., Ryerson F. J. and Peterson B. T. (2011) Influence of liquid structure on diffusive isotope separation in molten silicates and aqueous solutions. *Geochim. Cosmochim. Acta* **75**(11), 3103–3118.

Watkins J. M., Liang Y., Richter F., Ryerson F. J. and DePaolo D. J. (2014) Diffusion of multi-isotopic chemical species in molten silicates. *Geochim. Cosmochim. Acta* **139**, 313–326.

Watkins J. M., DePaolo D. J. and Watson E. B. (2017) Kinetic fractionation of non-traditional stable isotopes by diffusion and crystal growth reactions. *Rev. Mineral. Geochem.* **82**(1), 85–125.

Watson E. B. and Baxter E. F. (2007) Diffusion in solid-Earth systems. *Earth Planet. Sci. Lett.* **253**(3), 307–327.

Wu H. -J., He Y. -S., Teng F. -Z., Ke S., Hou Z. -H., Li S. -G. (2017) Diffusion-driven magnesium and iron isotope fractionation at a gabbro-granite boundary. Geochim. Cosmochim. Acta (in press). http://doi.org/10.1016/j.gca.2017.11.010.

Young E. D., Galy A. and Nagahara H. (2002) Kinetic and equilibrium mass-dependent isotope fractionation laws in nature and their geochemical and cosmochemical significance. *Geochim. Cosmochim. Acta* **66**(6), 1095–1104.

Associate editor: Frederic Moynier